Interdisciplinary Research in Medical Sciences Specialty
ISSN: 3062-4401
2026, Volume 6, Issue 1, Page No: 72-88

Available online at: www.galaxypub.co/page/journals

Galaxy Publication

Cross-Neutralizing Antibodies and NK Cell Immunity Underlie Protection against BA.5 Following Ad5-Boosted COVID-19 Vaccination

Peter Nilsson[1]*, Eva Johansson[1], Lars Andersson[2]

[1]Department of Virology and Vaccine Immunology, Faculty of Medicine, Karolinska Institute, Stockholm, Sweden.
[2]Department of COVID-19 Vaccine Research and NK Cell Biology, Faculty of Medicine, Lund University, Lund, Sweden.

***E-mail** ✉ peter.nilsson@ki.se

Received: 15 November 2025; **Revised:** 18 February 2026; **Accepted:** 24 February 2026

ABSTRACT

Throughout the COVID-19 pandemic, multiple vaccine platforms were employed across the globe. Nevertheless, the majority depended on immunogenicity data and bridging studies instead of direct retrospective evaluation derived from actual community infections. Consequently, knowledge regarding protective processes during natural exposure to circulating variants remained incomplete. A retrospective cohort analysis based on real-world BA.5 infections was performed to determine the protective performance of Ad5-nCoV booster immunization (A-A). In-depth multilayered immunological characterization was carried out, incorporating measurements of neutralizing antibodies (NAbs), single-cell B cell receptor (BCR) sequencing, transcriptomic analysis via RNA-seq, antibody-dependent cellular cytotoxicity (ADCC), natural killer (NK) cell cytotoxic function, and virus-specific T cell responses. Integration of these datasets enabled detailed dissection of the protective pathways activated by the A-A strategy. Administration of the A-A regimen achieved 48% effectiveness in preventing symptomatic BA.5 infection (115/239), in contrast to the 10% effectiveness observed with the three-dose inactivated vaccine schedule (I-I-I; 4/39). Among A-A recipients, 52% (124/239) developed symptomatic disease, 38% (90/239) showed asymptomatic infection, and 10% (25/239) stayed uninfected. Relative to the I-I-I cohort, participants in the A-A group displayed markedly elevated NAbs directed against BA.5 (GMT = 180 versus I-I-I GMT = 54) along with comparable titers against wild-type virus (GMT = 358 versus 226), even though anti-S IgG concentrations were lower (GMT = 6441 versus 12,228) two months after BA.5 infection. Single-cell BCR sequencing demonstrated a more diverse array of neutralizing antibody lineages in the A-A group, with prominent utilization of IGHV4-39 and higher levels of somatic hypermutation. In addition, transcriptomic data combined with functional testing indicated strengthened NK cell-driven ADCC activity and enhanced cytotoxicity toward K562 target cells in individuals who received the A-A booster. The Ad5-nCoV booster dose enhances protection from symptomatic BA.5 infection via the generation of cross-reactive neutralizing antibodies possessing greater epitope breadth and through augmentation of NK cell-mediated innate immune functions. This retrospective examination yields important information on the immunogenicity profiles and underlying molecular processes of two different vaccination regimens in the context of natural BA.5 infection. It underscores the value of Ad5-vector technology and supplies strategic direction for upcoming immunization policies targeting potential Disease X, while reinforcing the critical role of real-world retrospective evaluations in advancing vaccine science.

Keywords: Ad5-nCoV vaccine, Protective efficacy, BA.5 infection, Cross-neutralizing antibodies, NK cell immunity

How to Cite This Article: Nilsson P, Johansson E, Andersson L. Cross-Neutralizing Antibodies and NK Cell Immunity Underlie Protection against BA.5 Following Ad5-Boosted COVID-19 Vaccination. Interdiscip Res Med Sci Spec. 2026;6(1):72-88. https://doi.org/10.51847/kcACqjdXOL

Introduction

Following its initial appearance in December 2019, severe acute respiratory syndrome coronavirus 2 (SARS-CoV-2) initiated a worldwide pandemic marked by significant illness and death. In response to coronavirus disease

2019 (COVID-19), a wide range of vaccination programs were introduced internationally. Within mainland China, although inactivated vaccines had been administered on a large scale prior to December 2022, a major outbreak of Omicron BA.5/BF.7 variants took place toward the end of that year. Survey data showed that self-reported infections peaked between December 19 and 21, 2022, culminating in an overall infection rate of 82.4% across the Chinese population by February 7, 2023 [1]. Complementing the inactivated vaccines, the adenovirus type 5 (Ad5) vectored COVID-19 vaccine developed by CanSino Biologics in Tianjin, China, saw broad application. Adenoviral vector systems present notable benefits, including minimal pathogenicity, genomic safety, and absence of host genome integration [2, 3]. Beyond driving potent humoral responses, these vectors also promote cellular immunity required for the clearance of infected cells. A single intramuscular injection of the Ad5 vaccine produced strong immunogenicity, evidenced by RBD-specific IgG levels reaching a peak of 656.5 that endured for a minimum of 6 months [4, 5]. In a phase 3 trial, one dose of an Ad5 SARS-CoV-2 vaccine demonstrated 57.5% efficacy against PCR-positive COVID-19 and 91.7% efficacy against severe outcomes at 28 days post-vaccination [6]. An international phase 3 evaluation of the Ad26 SARS-CoV-2 vaccine similarly reported 66.1% efficacy against moderate-to-severe disease at 28 days, with protection rising to 85.4% for critical illness [7].

To strengthen immune responses, heterologous booster approaches have been explored. The Sputnik V heterologous regimen, which pairs Ad26 priming with Ad5 boosting, attained 91.6% efficacy against symptomatic PCR-confirmed COVID-19 and complete (100%) protection against moderate or severe forms [8]. Heterologous boosting using aerosolized Ad5-nCoV after primary inactivated vaccination also produced substantially superior neutralizing antibody responses compared with a homologous three-dose inactivated regimen [9-11]. Despite these encouraging data, the sustained protective capacity of an intramuscular Ad5-nCoV booster delivered roughly one year after initial immunization—particularly in relation to BA.5 infection—has not been comprehensively documented.

Several immunological elements shape the ability of wild-type (WT)-focused vaccines to guard against heterologous BA.5 infection. These include the extent of epitope overlap between WT and BA.5 antigens generated by each platform and the strength of NAbs recognizing those shared epitopes. The majority of existing research evaluates protection by measuring aggregate NAb titers toward variant strains [12-15]. Hybrid immunity arising from vaccination plus subsequent Omicron BA.1/BA.2 breakthrough infection, for instance, generates markedly higher BA.5-specific NAb levels than either vaccination or infection in isolation, resulting in improved cross-protection [14, 15]. Adenovirus-based vaccines possess distinctive immune-modulating features. In addition to stimulating vigorous T cell activity, their replication-incompetent nature can induce trained immunity within innate populations such as NK cells and monocytes—an attribute generally absent following three-dose inactivated vaccination [16-20]. Such differences may manifest as altered NK cell functions, including direct cytotoxicity and antibody-dependent cellular cytotoxicity (ADCC). NK cells are known to cooperate with vaccine-generated antibodies in infection control [21, 22]. Studies by Rahman and colleagues revealed that V1-deleted SIV/HIV vaccines elicit memory-like NK cell populations at mucosal and systemic sites. These trained NK cells were associated with decreased susceptibility to SIV/HIV infection and aligned with V2-specific ADCC responses, demonstrating their contribution to limiting viral acquisition [23]. Booster vaccinations further promote NK cells with a more differentiated phenotype and increased killing capacity relative to those elicited by primary immunization [24]. Nevertheless, the behavior of NK cells following BA.5 breakthrough infection and the persistence of hybrid immunity against newly emerging variants require further clarification.

Few studies have directly compared post-breakthrough immune responses across populations boosted with different regimens. The current investigation began with a side-by-side assessment of clinical features and antibody responses in individuals who received two doses of Ad5 vaccine versus three doses of inactivated vaccine, emphasizing protective outcomes. To uncover mechanisms responsible for the superior performance of the Ad5 booster, NAb titers and antigen-specific T cell immunity were quantified after BA.5 exposure. Memory B cells specific to BA.5 were then sorted for single-cell BCR sequencing to investigate clonal expansion and somatic mutation profiles. RNA-seq-based transcriptomic profiling compared overall immune states between the Ad5-boosted and inactivated-vaccine cohorts, supplemented by detailed functional evaluation of NK cell activity. Overall, this work delivers an original mechanistic exploration of Ad5 booster-mediated defense against BA.5 infection and examines the longevity of cross-variant immunity, thereby contributing a robust immunological foundation for the continued optimization of heterologous vaccination protocols.

Materials and Methods

Cohorts and sample collection

This investigation sought to determine the protective performance of the Ad5-nCoV vaccine (CanSino Biologics, Tianjin, China) in the setting of BA.5 breakthrough infection. A total of 239 participants who had completed two intramuscular doses of the Ad5-nCoV vaccine were enrolled (A-A group). Participants in this group had a median age of 53 years (IQR: 42–66), including 95 females (40%). Additionally, diabetes was reported in 10 individuals (4%) and hypertension in 79 (33%) **(Table 1)**. Peripheral blood samples for longitudinal immunogenicity evaluation were drawn at day 0 (D0), 1 month (1 M), and 3 months (3 M) following booster administration. After continued monitoring, specimens were also acquired at 2 months (2 M) following laboratory-confirmed BA.5 breakthrough infection **(Figure 1a)**.

A parallel comparator group consisted of 56 individuals who had received three doses of inactivated vaccines (CoronaVac; I-I-I group) and was included in the retrospective analysis. The inactivated vaccine was produced from the wild-type strain, with the third dose given 6 months after the second. To achieve balanced comparison with the A-A cohort, I-I-I participants were selected using predefined matching standards. All had finished the complete three-dose inactivated series (n = 15 at 1 M post-booster; n = 15 at 3 M post-booster), documented BA.5 breakthrough infection, and supplied samples at 2 months post-infection (n = 26), aligning with the corresponding time point in the A-A group **(Figure 1a and Table 2)**. This multi-phase sampling strategy facilitated a thorough examination of vaccine-generated immune responses and their relationship to protection from SARS-CoV-2 infection. To additionally investigate outcomes associated with the I-I-I regimen, a separate group of 39 participants was recruited, displaying a median age of 32 years (IQR: 29–34) and comprising 24 females (62%), **(Table 3)**.

Table 1. Demographic details and clinical profile of participants in the A-A group

From: Ad5-boosted COVID-19 vaccine reduces symptomatic BA.5 infection via cross-neutralizing antibodies and NK cell immunity

Characteristic	Category	Total (n = 239)	Uninfected (n = 25)	Asymptomatic (n = 90)	Symptomatic (n = 124)
Participants, n	—	239	25	90	124
Mean age (years)	—	—	59	52	53
Age group, n	18–39	50	1	21	28
	40–49	39	2	17	20
	50–59	60	10	26	24
	60–69	49	7	11	31
	>70	41	5	15	21
Sex, n (%)	Female	95 (40%)	6 (24%)	31 (34%)	58 (47%)
	Male	144 (60%)	19 (76%)	59 (66%)	66 (53%)
Comorbidities, n (%)	Diabetes	10 (4%)	1 (4%)	4 (4%)	5 (4%)
	Hypertension	79 (33%)	11 (44%)	28 (31%)	40 (32%)
	Hypertension and diabetes	12 (5%)	3 (12%)	3 (3%)	6 (5%)
Infection identification	Antigen test	—	Negative (−)	Negative (−)	Positive (+)
Clinical symptoms, n (%) *	Fever	78 (63%)	—	—	78 (63%)
	Fatigue	31 (25%)	—	—	31 (25%)
	Cough	49 (40%)	—	—	49 (40%)
	Muscle soreness	43 (35%)	—	—	43 (35%)
	Nasal congestion	13 (10%)	—	—	13 (10%)
	Sore throat	30 (24%)	—	—	30 (24%)
	Diarrhea	9 (7%)	—	—	9 (7%)

1. +: positive; −: negative

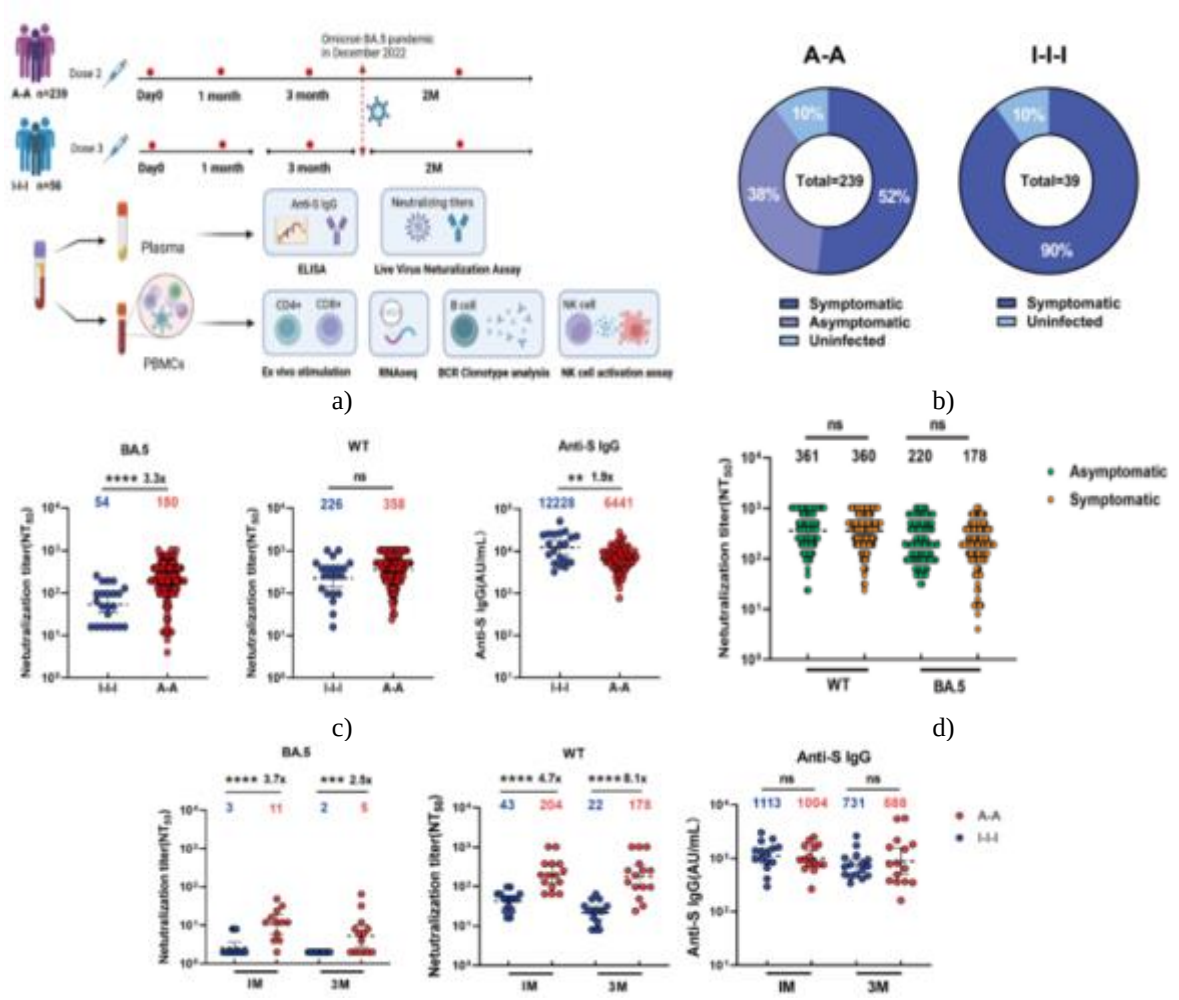

Figure 1. Immunogenicity profiles and protective performance of A-A compared with I-I-I during BA.5 infection.

a Overview of the longitudinal sample collection timeline for the A-A (n = 239) and I-I-I (n = 56) cohorts. b Proportions of symptomatic and asymptomatic infections observed in the A-A group. c Levels of anti-BA.5 and anti-WT neutralizing antibodies together with anti-S IgG in the A-A (n = 239) versus I-I-I (n = 26) groups at 2 months after BA.5 breakthrough infection. d Neutralizing antibody titers against BA.5 and WT strains in symptomatic (n = 124) versus asymptomatic (n = 90) A-A participants at 2 months post BA.5 breakthrough infection. e Geometric mean titers (GMT) for anti-BA.5 NAbs, anti-WT NAbs, and anti-S IgG measured at 1 month and 3 months after booster vaccination in both groups (n = 15). At 1 month post-booster, 80% of I-I-I samples registered anti-BA.5 titers below the lower detection limit (4) and were assigned the value 2. All I-I-I samples at 3 months post-booster were below the detection limit (4) and likewise assigned the value 2. Dotted lines denote the geometric mean accompanied by 95% confidence intervals. Statistical comparisons between groups were conducted using the Mann–Whitney test (*P < 0.05, **P < 0.01, ***P < 0.001, ****P < 0.0001).

Table 2. Details of I-I-I vaccinated participants with subsequent BA.5 infection
From: Ad5-boosted COVID-19 vaccine reduces symptomatic BA.5 infection via cross-neutralizing antibodies and NK cell immunity

Characteristic	I-I-I, 1 Month Post-Booster *(n = 15)*	I-I-I, 3 Months Post-Booster *(n = 15)*	I-I-I, 2 Months Post-BA.5 Infection *(n = 26)*
Participants, n	15	15	26
Mean age (years)	38	34	58
Sex, n (%)			
Female	12 (80%)	11 (73%)	13 (50%)

Male	3 (20%)	4 (27%)	13 (50%)
Infection status			
SARS-CoV-2 antigen test	Negative (−)	Negative (−)	Positive (+)

1. +: positive; −: negative

Table 3. Clinical characteristics of I-I-I recipients following BA.5 infection
From: Ad5-boosted COVID-19 vaccine reduces symptomatic BA.5 infection via cross-neutralizing antibodies and NK cell immunity

Characteristic	Category	Symptomatic (n = 35)	Uninfected (n = 4)	Total (n = 39)
Participants, n	—	35	4	39
Mean age (years)	—	31	40	32
Sex, n (%)	Female	21 (60%)	3 (75%)	24 (62%)
	Male	14 (40%)	1 (25%)	15 (38%)
Infection status	SARS-CoV-2 antigen test	Positive (+)	Negative (−)	—
Clinical symptoms, n (%) *	Fever	31 (89%)	—	—
	Fatigue	8 (23%)	—	—
	Cough	28 (80%)	—	—
	Muscle soreness	15 (43%)	—	—
	Nasal congestion	22 (63%)	—	—
	Sore throat	26 (74%)	—	—
	Diarrhea	3 (9%)	—	—

1. +: positive; −: negative

This research protocol was reviewed and monitored by the GMUH Ethics Committee (No.2021–78).

Enzyme-linked immunosorbent assay (ELISA)

Quantification of spike (S) protein-specific binding antibodies in plasma obtained from vaccinated participants and those with breakthrough infection relied on an indirect ELISA approach. Microtiter plates (96-well) were first coated overnight at 4 °C with wild-type (WT) SARS-CoV-2 S protein. Blocking was achieved the next day using 3% milk prepared in phosphate-buffered saline (PBS). A plasma pool with elevated anti-S reactivity functioned as the reference standard, assigned an arbitrary value of 2000 AU/mL. Each plate incorporated a twofold dilution series of this standard to produce a calibration curve. Experimental samples, diluted 1:100, were incubated in the wells for 1 h. HRP-labeled secondary antibody (109–035–088, Jackson ImmunoResearch Laboratories) was then applied for 1 h at 37 °C. After repeated washing, 100 µL TMB stabilized chromogen (Invitrogen, USA) was introduced, with color development allowed for 10 min at 37 °C prior to termination by 50 µL stopping solution (R&D Systems, USA). Absorbance at 450 nm was recorded on a Multiskan GO spectrophotometer (Thermo Fisher Scientific, Waltham, MA, USA). Sample concentrations were calculated from logistic regression-fitted standard curves.

Peripheral blood mononuclear cell (PBMC) isolation and ex vivo stimulation

Isolation of PBMCs from heparinized blood was carried out by Ficoll–Paque density gradient centrifugation (GE Healthcare, Cat# 17–1440–02). For stimulation experiments, 5 × 10^5 cells were exposed separately to peptide pools spanning the S1 subunit (171 15-mer peptides), S2 subunit (145 15-mer peptides), or a pooled combination of membrane, nucleocapsid, and envelope proteins (N/M/E; 171 15-mer peptides). These incubations occurred in RPMI 1640 medium (Gibco) enriched with 10% heat-inactivated FBS (Biological Industries, Israel Beit-Haemek), 100 U/ml penicillin (Gibco), 0.1 mg/ml streptomycin (Gibco), 10 U/ml rIL-2, and 1 µM GolgiPlug (BD Biosciences, San Diego, CA) for 24 h under standard culture conditions (37 °C, 5% CO2). Matched control cultures received identical medium with 0.01% DMSO (Sigma) in the absence of peptides.

Flow cytometry

Post-stimulation cells were viability-stained for 15 min at room temperature with LIVE/DEAD® Fixable Aqua Dead Cell Stain (Thermo Fisher Scientific, Cat #L34957). Surface immunophenotyping followed for 30 min in the dark at room temperature using BV605 anti-CD3 (BD Pharmingen™, Clone SP34-2, Cat#562,994), BV786 anti-CD4 (BD Pharmingen™, Clone SK3, Cat#563,877), and AF488 anti-CD8 (BD Pharmingen™, Clone RPA-T8, Cat#557,696). Fixation and permeabilization were conducted on ice for 15 min with Cytofix/Cytoperm™

reagent (BD Bioscience, Cat# 554,714). Subsequent intracellular staining for 30 min on ice targeted TNF-α (PE-Cy7, BD Clone MAb11, Cat# 557,647) and IFN-γ (APC, BD Pharmingen™ Clone B27, Cat# 554,702). Samples were resuspended in 200 µl FACS buffer, acquired on a BD LSRFortessa X-20 instrument (BD Bioscience), and evaluated using FlowJo software (Treestar).

SARS-CoV-2 conventional virus neutralization test

Plasma neutralizing activity against SARS-CoV-2 was determined via a CPE-based microneutralization assay as outlined earlier [25]. Starting at a 1:4 dilution, plasma underwent eight additional twofold dilution steps. Diluted plasma was combined with 100 TCID50 of either WT or Omicron BA.5 virus stocks in 96-well format and pre-incubated for 2 h at 37 °C, 5% CO2. Vero E6 cells (1.2 × 10^4 per well) were then added, followed by 4 days of incubation under the same conditions. CPE readout was performed with a Celigo Imaging Cytometer and interpreted against high-neutralizing positive control plasma and negative controls (seronegative serum and uninfected cells). The assay's detection limit was 4, with titers below this threshold recorded as an NT50 value of 2.

RNA extraction and quantification of gene expression

Bulk RNA sequencing served to delineate transcriptomic differences in systemic immune responses after BA.5 infection between A-A and I-I-I vaccinated individuals. This analysis focused on generating global expression profiles of immunity-associated genes, pinpointing DEGs across cohorts, and uncovering pathways linked to differential protective outcomes. Nine PBMC samples were randomly chosen from each group, ensuring verified BA.5 breakthrough infection and comparable demographic features. Frozen samples were thawed rapidly at 37 °C, rinsed with PBS, and subjected to total RNA isolation with the Eastep® Super Total RNA Extraction Kit (Shanghai Promega, Cat# LS1040) per the supplier's protocol. Sequencing services, including library construction and data processing, were outsourced to Genedenovo (Guangzhou).

RNA-sequencing and differentially expressed gene analysis

Libraries for RNA sequencing were generated from total RNA using the Eastep® Super Total RNA Extraction Kit (Shanghai Promega, catalog number LS1040) as specified by the manufacturer. These libraries were sequenced on the Illumina NovaSeq 6000 system in paired-end mode with 150 bp read length. The quality of the obtained FASTQ files was examined using FastQC from Babraham Bioinformatics [26]. Adapter trimming and removal of low-quality bases from the raw reads were carried out with cutadapt [27]. Alignment of the filtered reads to the human reference genome GRCh38, along with the GTF annotation file from GENCODE release 45, was performed using STAR software (version 2.7.10b) [28]. Following index building, gene-level read counts were obtained through the "-quantMode GeneCounts" setting. Differential expression analysis was executed with DESeq2 based on the STAR-derived counts. Genes showing an adjusted P-value < 0.05 and $|\log_2$ fold change$| >$ 0.5 were designated as differentially expressed. Enrichment of Gene Ontology (GO) terms was assessed via the g:Profiler web tool [29]. Results from the RNA-seq pipeline were visualized with the SRplot online platform [30].

Isolation of SARS-CoV-2 spike-specific memory B cells

BA.5 spike protein was labeled with biotin employing the EZ-Link Sulfo-NHS-LC-Biotinylation Kit (Cat# 21327) at a 1:1.3 molar ratio. Tetrameric probes were assembled by mixing the biotinylated spike with streptavidin-PE (SA-PE; Invitrogen, Cat# S866) at a 4:1 ratio and incubating for 30 min at room temperature. Cryopreserved PBMCs were thawed and treated with Fixable Viability Stain 510 (BD Horizon™, Cat# 564406) for 15 min at room temperature. Following one wash in FACS buffer, cells were incubated with the spike-specific tetramer for 60 min at 4 °C in darkness. After washing, multi-color surface staining was conducted for 20 min at room temperature using PE-Cy7 anti-CD3 (BD Pharmingen™, Clone HIT3a, Cat# 563423), APC-Cy7 anti-CD19 (BioLegend, Clone HIB19, Cat# 302218), PerCP/Cyanine 5.5 anti-CD27 (BioLegend, Clone M-T271, Cat# 560612), and FITC anti-IgG (BioLegend, Clone HP6017, Cat# 409310). Viable single spike-specific memory B cells ($CD3^-CD19^+CD27^+IgG^+S^+$) were sorted into 96-well plates on a BD Aria III flow cytometer (BD Biosciences).

BCR repertoire analysis

RNA from individually sorted B cells was reverse-transcribed with SuperScript IV VILO Master Mix (Thermo Fisher, Cat# 11754250) following the provided protocol. One microgram of cDNA served as input for nested PCR amplification of immunoglobulin heavy and light chain variable domains using PrimeSTAR Max DNA Polymerase (Takara). Correctly sized products were gel-extracted and subjected to deep sequencing. Raw data were analyzed through the IMGT database [31] to determine V/J gene usage, CDR3 sequences, and levels of somatic hypermutation. Given the unequal sequence yields between the A-A and I-I-I groups, group comparisons of repertoire features were performed with the Wilcoxon test for unpaired samples. Clonotypes were identified by shared V and J segments plus identical HCDR3 amino acid sequences. Sequence identity calculations and alignment analyses were conducted using Biostrings v2.60.2 in R. HCDR3 regions from paired heavy-light chains were matched to entries in the CoV-AbDab database via Hamming distance; sequences of matching length with ≥70% amino acid identity were clustered together. Repertoire diversity and clonal expansion patterns were evaluated by assessing the distribution and frequency of these clonotypes.

ADCC NK cell activation assay

The ability of NK cells to perform antibody-dependent cellular cytotoxicity (ADCC) against SARS-CoV-2 spike was tested in donors from the A-A and I-I-I cohorts. Plates were coated with SARS-CoV-2 S protein, and plasma from a confirmed IgG-positive individual was added for 2 h at 37 °C. After washing away unbound plasma components, 2×10^5 PBMCs from study participants were introduced and incubated for 5 h at 37 °C under 5% CO_2. During incubation, APC anti-CD107a (Pharmingen, Cat# 560664), brefeldin A, and monensin (BD Biosciences) were present. Cells were subsequently labeled with FITC anti-CD3 (BD Biosciences, Clone HIT3a, Cat# 561802) and PE-Cy7 anti-CD56 (BD Biosciences, Clone B159, Cat# 557747) for 30 min at 4 °C. Following permeabilization with Cytofix/Cytoperm (BD Biosciences, Cat# 554714), intracellular IFN-γ was detected with PE anti-IFN-γ (BD Biosciences, Clone B27, Cat# 559327). Flow cytometry data were collected on a BD LSRFortessa X-20 (BD Biosciences) and processed in FlowJo (Tree Star).

NK cell cytotoxicity assay

Cytotoxic function of NK cells was quantified using K562 cells, which lack MHC class I expression, as targets in a flow-based assay. NK cells were purified from PBMCs by CD56-positive magnetic selection (Miltenyi Biotec, Cat# 130-050-401). Target cells were stained with CFSE for 10 min at 37 °C. Effector and target cells were combined at a 5:1 ratio in V-bottom plates, spun down at 200 g for 3 min, and cultured for 12 h at 37 °C with 5% CO_2. Post-incubation, cells were stained with 7-AAD and PE Annexin V (BD Pharmingen, Cat# 559763). Acquisition was performed on a BD LSRFortessa X-20 instrument (BD Biosciences). Percent cytotoxicity was determined by calculating the fraction of $CFSE^+$ Annexin V^+ target cells after subtracting spontaneous death observed in target-only controls.

Statistical analysis

Analyses of antibody levels, T cell responses, and NK cell effector functions were conducted in GraphPad Prism version 6.0 (GraphPad Software, USA). Clonality parameters within BCR repertoires were examined using the Biostrings v2.60.2 package in R. Statistical significance was defined as $P < 0.05$.

Mann–Whitney tests were applied for between-group comparisons of antibody titers, T cell responses, and NK cell activities. Wilcoxon rank-sum tests were utilized for BCR sequence characteristics, consistent with R package standards. Antibody titers are summarized as geometric mean titers (GMT) with 95% confidence intervals (CI). T cell and NK cell data are expressed as mean values ± standard error of the mean (SEM).

Results and Discussion

Ad5-boosted caccination reduced symptomatic BA.5 infections compared with three doses of inactivated vaccine

During the BA.5 outbreak in China, real-world protective efficacy of the Ad5 booster was tracked. Surveillance data indicated that 52% (124/239) of A-A recipients developed confirmed BA.5 infection with at least one classic symptom according to self-reported questionnaires **(Table 1)**; such cases were recorded as symptomatic infections. A BA.5-specific NAb titer threshold of 32 was applied to separate asymptomatic infection from the uninfected state. This cutoff was calculated from the geometric mean ± 3 standard deviations of anti-BA.5 NAb titers measured in the A-A cohort three months after booster immunization. Results showed that 38% (90/239) of

participants possessed anti-BA.5 NAb titers ≥ 32 without any symptoms and were therefore classified as asymptomatically infected. The final 10% (25/239) had titers < 32 and no symptoms, placing them in the uninfected category **(Figure 1b)**. In the I-I-I group, however, 90% (35/39) suffered symptomatic BA.5 infection, with only 10% (4/39) remaining uninfected **(Figure 1b and Table 3)**. Overall, the A-A regimen conferred stronger protection against symptomatic disease than the I-I-I schedule, although both approaches demonstrated comparable and modest efficacy in completely preventing infection.

Ad5-boosted vaccination produced markedly elevated anti-BA.5 NAbs, equivalent anti-WT NAbs, and decreased anti-S IgG titers after BA.5 infection relative to I-I-I

To clarify whether superior heterologous protection by the Ad5 booster stemmed from distinct immune profiles, antibody responses—including anti-S IgG and neutralizing antibodies to WT and BA.5—were compared in infected individuals from both vaccination groups. At two months following BA.5 infection, anti-BA.5 NAb geometric mean titers were 3.3-fold higher in the A-A group (180, 95% CI 146–221) than in the I-I-I group (54, 95% CI 35–83; P < 0.0001). Anti-WT NAb levels did not differ significantly (358, 95% CI 307–419 in A-A versus 226, 95% CI 138–372 in I-I-I; P = 0.0604), but anti-S IgG concentrations were substantially lower in A-A recipients (6441 AU/ml, 95% CI 5545–7482) compared with I-I-I (12,228 AU/ml, 95% CI 8420–17,759; P = 0.0032) at the same interval **(Figure 1c)**. Within the A-A group, NAb titers against WT and BA.5 showed no meaningful distinction between symptomatic and asymptomatic cases **(Figure 1d)**. Titers also remained consistent regardless of gender, age, or comorbid conditions. These patterns confirm that the A-A strategy generated more robust cross-neutralizing responses to WT and BA.5 strains than the I-I-I regimen at two months post infection.

Prior studies have established that WT-based vaccines typically produce very low BA.5-neutralizing activity six months after immunization [32-35]. Building on the post-infection observation of stronger cross-reactivity in A-A recipients, pre-exposure NAb levels were examined. The A-A regimen induced higher anti-BA.5 NAb titers at both one and three months after vaccination than I-I-I **(Figure 1e)**. Geometric mean titers at one month were 11 (95% CI 7–24) in A-A versus 3 (95% CI 2–5) in I-I-I. By three months, titers in the I-I-I group had dropped below detection limits, whereas A-A maintained a titer of 5 (95% CI 1–21). Anti-WT NAb responses were also stronger in A-A, reaching 4.7-fold and 8.1-fold higher levels at one and three months post booster, respectively **(Figure 1e)**. Anti-S IgG levels remained similar between groups after vaccination **(Figure 1e)**. Although the three-month difference in anti-BA.5 NAbs was modest, when viewed alongside post-infection data **(Figure 1c)**, the findings indicate that A-A more efficiently drives cross-reactive neutralizing antibodies against WT and BA.5.

Ad5 booster vaccine drives stronger neutralizing antibody responses by enhancing BCR diversity, extending CDR3 length, and elevating somatic hypermutation after BA.5 infection

To evaluate whether improved protection by A-A extended beyond simple titer increases to greater clonal diversity, BCR repertoires were profiled in S-specific memory B cells at two months after BA.5 breakthrough infection. Cells were isolated via BA.5 S-tetramer staining using the $CD3^{-}CD19^{+}CD27^{+}IgG^{+}S^{+}$ gating strategy **(Figure 2a)**. Single-cell multiplex PCR was performed to characterize BCR usage. IGHV gene distribution is depicted for I-I-I (blue) and A-A (red) in **Figure 2b**. Both groups utilized several IGHV families, including IGHV1 (e.g., IGHV1-3, IGHV1-69), IGHV3 (e.g., IGHV3-7, IGHV3-30), and IGHV4 (e.g., IGHV4-39, IGHV4-59). The A-A group, however, exhibited a wider and less focused IGHV gene usage pattern. IGHV4-39 accounted for 9% of sequences in A-A, while IGHV3-30 represented 16% in I-I-I **(Figure 2b)**. This broader IGHV profile indicates higher BCR diversity in the A-A cohort. CDR3 lengths were also slightly extended in A-A compared with I-I-I (P = 0.049)**(Figure 2c)**, potentially allowing recognition of a wider array of viral epitopes.

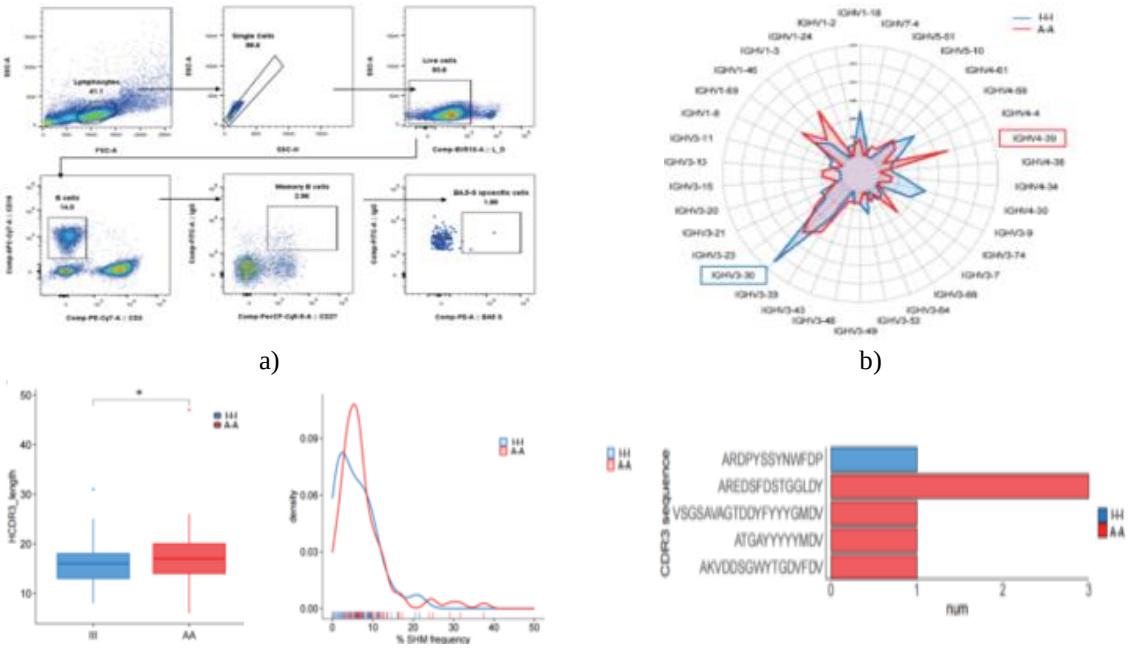

Figure 2. BCR repertoire characteristics and clonal properties in A-A versus I-I-I participants at 2 months following BA.5 breakthrough infection. a) Strategy for flow cytometric sorting of S-specific B cells. b) Frequency of immunoglobulin heavy chain variable region (IGHV) gene usage in the two groups. c) Complementarity-determining region 3 (CDR3) length profiles among B cells secreting anti-BA.5 antibodies. d) Examples of CDR3 amino acid sequences derived from major neutralizing clones. e) Levels of somatic hypermutation (SHM) within BCRs, demonstrating markedly increased mutation rates in A-A recipients. Statistical comparison of mutation frequencies was performed using the Wilcoxon rank-sum test (*P < 0.05).

Matching of CDR3 sequences to the CoV-AbDab database revealed a significantly larger number of matches to known neutralizing antibodies in the A-A group than in I-I-I **(Figure 2e)**. This suggests the Ad5 booster promotes development of a more intricate and broadly reactive antibody repertoire. Somatic hypermutation is a key process for antibody affinity maturation, and the A-A group displayed notably higher SHM rates **(Figure 2d)**. This enhanced mutation frequency reflects more advanced B cell maturation, enabling production of high-affinity antibodies with potent neutralizing capability against SARS-CoV-2 variants. These immunological features provide a mechanistic explanation for the Ad5 booster's improved performance, linking protection to both quantitative increases in NAbs and qualitative improvements in repertoire diversity and affinity.

Ad5 booster vaccination in conjunction with BA.5 infection augments innate immunity via elevated expression of NK cell-related genes

Bulk RNA sequencing was performed on PBMCs obtained from A-A (n = 9) and I-I-I (n = 9) participants at 2 months after BA.5 infection to compare the post-infection immune profiles between the two vaccination approaches. GO enrichment analysis, conducted through the "Wei Sheng Xin" online bioinformatics resource [30], indicated that genes upregulated in the A-A group were mainly enriched in innate immunity-related pathways. These included NK cell-mediated immunity, cytotoxic mechanisms, and broader leukocyte immune responses **(Figure 3a)**. Targeted inspection of NK cell-associated genes demonstrated significantly increased expression of NCR1, NCR3, PRF1, GZMB, KIR3DL1, KIR3DL2, and KIR3DL3 in individuals who received the Ad5 booster compared with the I-I-I group **(Figure 3b)**. Such results suggest that prior Ad5 boosting strengthens innate immune pathways, notably those governing NK cell activation and effector functions, thereby contributing to better control of BA.5 infection.

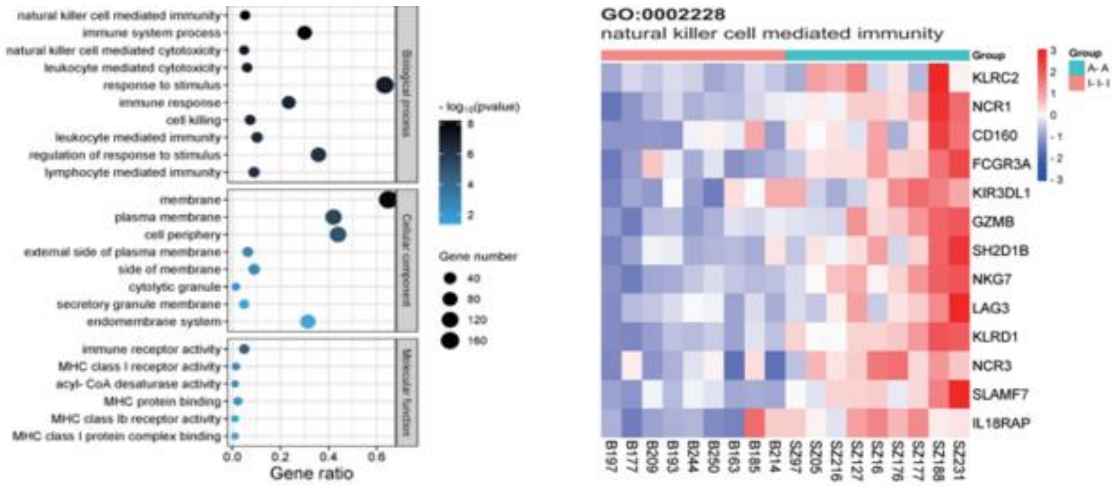

a) b)

Figure 3. Analysis of functional enrichment among differentially expressed genes (DEGs) in A-A versus I-I-I participants. b Heatmap displaying expression patterns of genes linked to NK cell activation and cytotoxicity.

Ad5 booster vaccination in conjunction with BA.5 infection promotes heightened NK cell-mediated ADCC activity and cytotoxic capability

To ascertain the involvement of NK cells in the superior protection afforded by the A-A strategy, functional assays were used to measure NK cell ADCC responses through detection of $CD107a^+$ and/or IFN-γ^+ NK cells **(Figure 4a)**. While the frequency of $CD107a^+$ NK cells did not differ significantly between groups (20.0%, 95% CI 15.0–25.0% in A-A versus 14.3%, 95% CI 11.1–17.5% in I-I-I; (**Figure 4b)**, left panel), the A-A group exhibited a clear increase in IFN-γ-producing NK cells (8.3%, 95% CI 4.3–12.3% versus 2.3%, 95% CI 1.2–3.4% in I-I-I; **(Figure 4b)**, middle panel). The population of double-positive IFN-$\gamma^+CD107a^+$ NK cells was 2.4 times higher in A-A recipients **(Figure 4b)**(right panel).

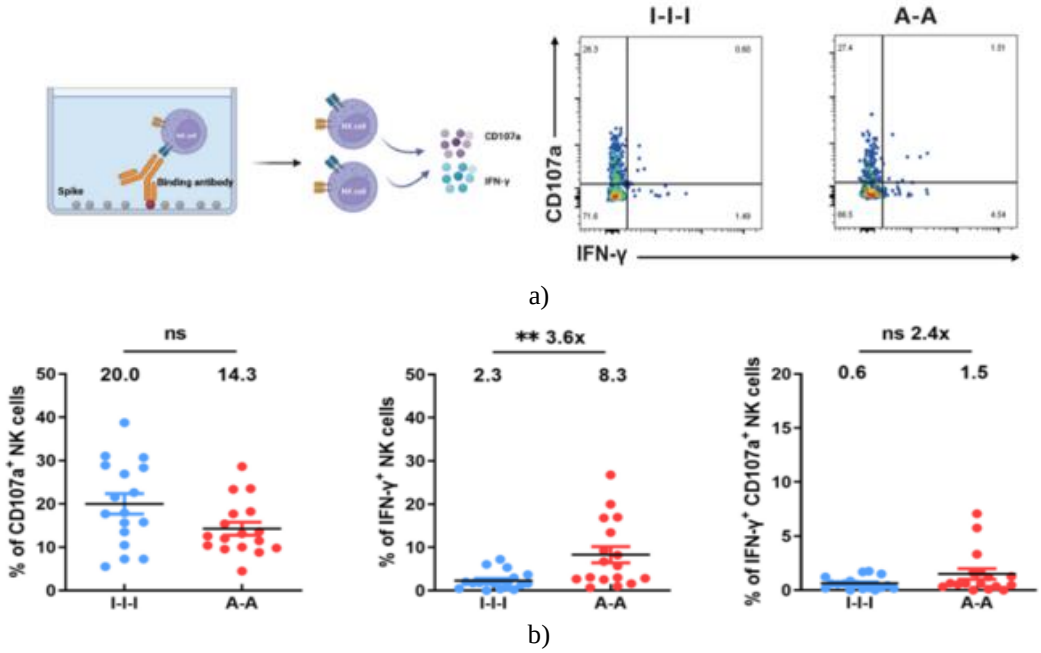

a)

b)

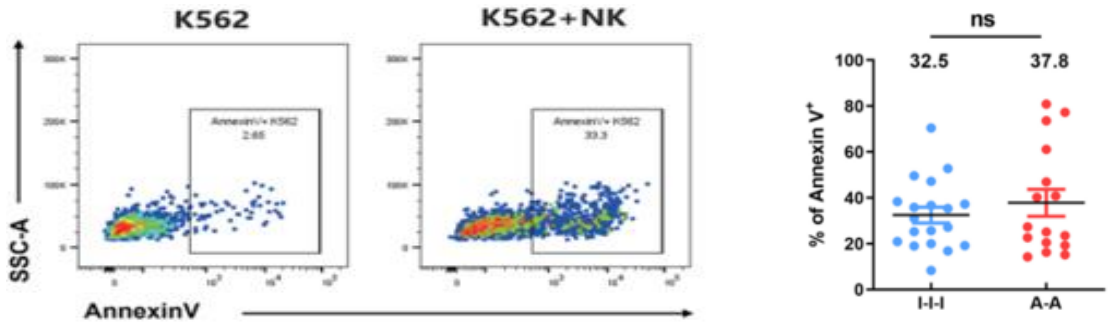

c) d)

Figure 4. Elevated NK cell ADCC responses and cytotoxic potential in A-A individuals.
a) Experimental design for NK cell stimulation using SARS-CoV-2 S protein and subsequent analysis of CD107a and IFN-γ expression. b) Proportions of IFN-γ^+ NK cells, CD107a$^+$ NK cells, and IFN-γ^+CD107a$^+$ NK cells across A-A and I-I-I groups (n = 17 per group). c) Representative flow cytometry plots of Annexin V$^+$/7-AAD$^+$ K562 target cells killed at a 5:1 effector-to-target ratio. d) Cytotoxicity quantification indicating a tendency for greater target cell lysis in the A-A group relative to I-I-I (n = 17 per group). Statistical comparisons between groups were performed with the Mann–Whitney test; ns, not significant; **P < 0.01.

Assessment of NK cell intrinsic cytotoxicity against K562 targets similarly showed a non-significant trend toward improved killing activity in the A-A group at 2 months post BA.5 infection (37.8% versus 32.5% in I-I-I); **(Figures 4c and 4d)**. Although this difference did not reach statistical significance, it corresponds with the heightened activation profile seen in the ADCC assay **(Figure 4b)**. Taken together, these data indicate that the Ad5 booster, when followed by BA.5 infection, bolsters both antibody-dependent and direct cytotoxic functions of NK cells, emphasizing the broad role of innate immunity in mediating the enhanced protection associated with the A-A vaccination approach.

BA.5 infection in individuals receiving Ad5 booster vaccination induced weaker virus-specific CD4$^+$ and CD8$^+$ T cell responses

As a viral vector vaccine, the Ad5 booster is anticipated to generate robust T cell immunity. Because the Ad5 construct encodes the full-length spike protein while the inactivated vaccine includes the complete set of SARS-CoV-2 proteins, T cell responses directed against S1, S2, and non-structural (N/M/E) proteins were evaluated separately. Virus-specific T cell activity was measured by detection of IFN-γ-producing CD4$^+$ and CD8$^+$ T cells **(Figure 5a)**. The I-I-I group displayed significantly stronger S1- and S2-specific IFN-γ^+ CD4$^+$ T cell responses than the A-A group, corresponding to 1.9-fold and 2.8-fold higher levels, respectively, with a similar trend observed in percentages. Responses against N/M/E proteins were also markedly elevated in the I-I-I group (0.09, 95% CI 0.03–0.15 versus 0.02, 95% CI 0.01–0.03 in A-A); **(Figure 5b)**. Overall, the numbers of S1-, S2-, and N/M/E-specific IFN-γ^+ CD4$^+$ T cells were 1.9-fold, 2.8-fold, and 6.8-fold higher, respectively, in I-I-I recipients compared with A-A **(Figure 5b)**. These data indicate that the A-A regimen elicits comparatively limited virus-specific CD4$^+$ T cell activation following BA.5 infection.

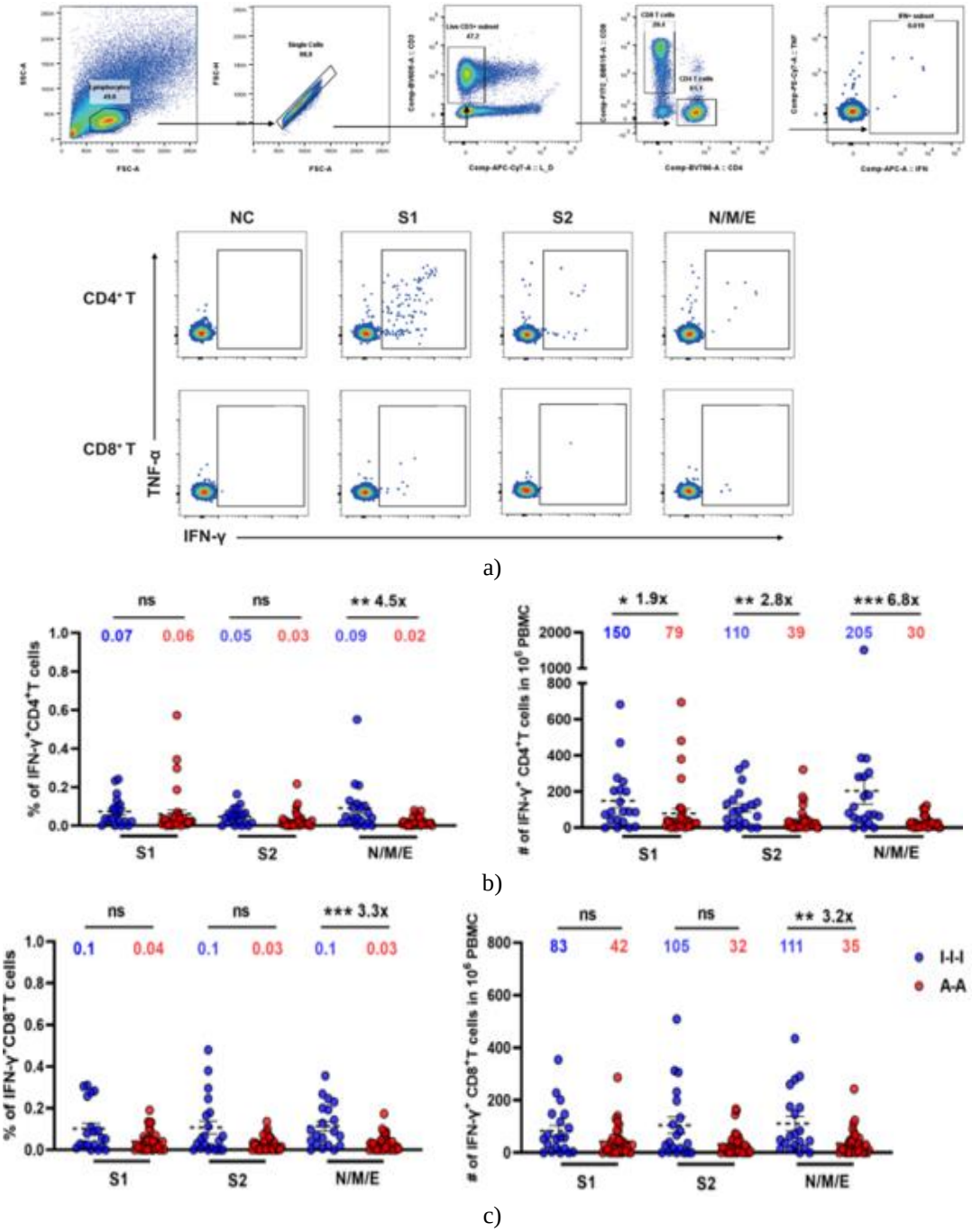

Figure 5. BA.5 infection following Ad5 booster vaccination resulted in diminished virus-specific CD4⁺ and CD8⁺ T cell responses.

A Flow cytometry gating approach and experimental outline for ex vivo stimulation of PBMCs with peptide pools derived from S1, S2, and N/M/E proteins, followed by intracellular cytokine staining to identify cytokine-producing CD4⁺ and CD8⁺ T cells. B Percentages (left) and absolute counts per million PBMCs (right) of IFN-γ⁺ CD4⁺ T cells in A-A and I-I-I groups at 2 months post BA.5 infection (n = 35 in A-A, n = 20 in I-I-I). C Percentages (left) and absolute counts per million PBMCs (right) of IFN-γ⁺ CD8⁺ T cells in A-A and I-I-I groups at 2 months post BA.5 infection (n = 35 in A-A, n = 20 in I-I-I). The Mann–Whitney test was used to evaluate differences in T cell responses between groups; ns, not significant; **P < 0.01, ***P < 0.001.

Comparable results were obtained for CD8⁺ T cells, with no significant differences in S1- or S2-specific IFN-γ⁺ CD8⁺ T cell frequencies or counts between the two groups. However, N/M/E-specific IFN-γ⁺ CD8⁺ T cell responses were substantially higher in the I-I-I group, showing 3.3-fold and 3.2-fold increases in percentage and cell number, respectively **(Figure 5c)**. These patterns suggest that memory T cells recognizing conserved non-

spike antigens (such as N, M, and E proteins) are more effectively recalled by inactivated vaccines upon subsequent BA.5 exposure.

While adenovirus vector vaccines have been extensively evaluated for immunogenicity, analyses based on real-world clinical infection outcomes remain relatively scarce. The current investigation showed that, within the A-A cohort, 52% of participants developed symptomatic BA.5 breakthrough infection, 38% experienced asymptomatic infection, and 10% stayed uninfected throughout the observation period. Notably, the symptomatic infection rate in this group was markedly lower than the 90% observed in the I-I-I group and the national estimate for China (exceeding 80%), where symptomatic cases accounted for 73% of infections [1, 36]. These observations emphasize the capacity of the Ad5 vaccine to curtail SARS-CoV-2 spread. Relative to a three-dose regimen of inactivated vaccine, administration of two Ad5 booster doses resulted in elevated BA.5-specific neutralizing antibody titers both in the immediate post-vaccination phase and following breakthrough infection. Of particular importance, the Ad5 platform generated antibodies recognizing a more diverse array of neutralizing epitopes and potentiated NK cell-mediated cytotoxicity along with ADCC functions. The integration of these enhanced adaptive and innate immune components underlies the greater protective effectiveness of the Ad5 platform against BA.5.

Findings from this study indicate that the A-A schedule generated substantially greater levels of anti-BA.5 NAbs compared with the I-I-I schedule. The A-A approach relies on E1/E3-deleted Ad5 vectors for expression of the SARS-CoV-2 S protein [37], a strategy recognized for stimulating robust humoral and cellular immunity [38]. Structural characterizations indicate that S proteins produced via Ad5 are prominently displayed on cellular membranes [39], thereby improving presentation of conserved antigenic epitopes shared across WT and BA.5 variants. Due to the replication-defective nature of the Ad5 vector, it yields higher amounts of endogenous and soluble antigens than the inactivated vaccine regimen. This facilitates more effective antigen capture and processing by APCs, including dendritic cells and macrophages, leading to strong engagement of both MHC class I and II pathways. Such processes enable efficient cross-presentation of S protein-derived peptides [40] and support the activation of CD8+ and CD4+ T cells, which in turn promote B cell maturation and affinity maturation. As a result, this leads to the development of high-affinity antibodies specific for conformation-sensitive neutralizing epitopes [41]. These mechanistic insights are reinforced by the markedly higher anti-BA.5 NAb titers detected in A-A recipients. At 1 month after vaccination, participants in the A-A group showed measurable anti-BA.5 NAbs (GMT = 11) exceeding the lower limit of detection [4], in contrast to the I-I-I group, where titers remained undetectable (GMT = 3). This advantage persisted, with A-A demonstrating 3.3-fold higher BA.5-specific NAb titers at 2 months after breakthrough infection, together with elevated frequencies of BA.5 S-specific memory B cells and IgG subclass antibodies.

Neutralizing antibody responses elicited by A-A versus I-I-I immunization exhibited differences not only in magnitude against BA.5 and WT strains **(Figure 1)** but also in underlying BCR repertoire selection and the extent of somatic hypermutation associated with affinity maturation. The A-A regimen further improves NAb functional quality by increasing SHM levels within B cell lineages, a key step in optimizing antibody binding to conserved neutralizing sites [41, 42]. In particular, A-A drove selective expansion of B cell clones utilizing the IGHV4-39 germline segment, which is linked to high-potency RBD-targeting antibodies effective against diverse SARS-CoV-2 variants [43]. The A-A group also showed enrichment of IGHV1-69, a germline known to recognize the L452R substitution characteristic of many Omicron sublineages [44]. Conversely, responses in the I-I-I group were dominated by antibodies derived from the IGHV3-30 germline. Although IGHV3-30 is frequently utilized in convalescent individuals and displays strong RBD binding, its relatively low SHM rate and tendency toward S2-region specificity reduce its utility against variant strains [45-47]. Structural evidence indicates that antibodies encoded by IGHV3-30 suffer substantial loss of neutralizing capability against Omicron subvariants due to epitope modifications [48]. Consequently, even though the I-I-I regimen produced elevated anti-S IgG levels (GMT = 12,228 compared with 4,694 in A-A), it proved inadequate in generating effective BA.5-specific NAbs. Taken together, these data illustrate that the enhanced neutralizing performance of A-A against BA.5 results from its distinctive promotion of BCR diversity, extended CDR3 regions, and SHM-facilitated antibody refinement.

NK cells play a pivotal role as frontline defenders in viral infections, exerting influence through immediate cytotoxic killing and cytokine-mediated signaling, as evidenced in infections with herpesviruses and Hantavirus [49, 50]. In addition to these direct effects, NK cells help shape adaptive antiviral responses by releasing IFN-γ, IP-10, MIP-1α, and MIP-1β, thereby restricting viral propagation and recruiting other immune effectors [51]. Growing research supports the concept of “trained immunity” within the NK cell compartment, whereby innate

cells acquire enhanced responsiveness to future pathogen encounters [52]. The Ad5-boosted vaccine illustrates this principle, with its adenoviral components engaging innate sensors such as TLRs and cytosolic DNA recognition pathways to induce cytokine environments that foster sustained NK cell adaptation [53]. Within the A-A cohort, trained immunity manifested as prolonged elevation of activation markers (NCR1, NCR3, CD160) and cytotoxic effectors (PRF1, GZMB), correlating with improved target cell killing. Ad5 immunization triggers epigenetic modifications and shifts in cellular metabolism within NK cells, equipping them for accelerated responses upon viral rechallenge. These conditioned NK cells display strengthened ADCC capacity, demonstrated by upregulated FCGR3A (CD16) and enhanced degranulation. Unlike the short-lived NK cell stimulation induced by inactivated vaccines, Ad5 establishes long-lasting NK memory populations, with both cytotoxic and cytokine-secreting subsets remaining functional beyond 6 months post-vaccination [54]. In summary, Ad5-elicited trained NK cells significantly contribute to the comprehensive protective effects observed against BA.5.

Limitations

This study presents several limitations. First, the relatively small number of participants in the I-I-I group may have compromised statistical power and reduced the external validity of between-group comparisons. Such sample size imbalance between the I-I-I and A-A cohorts could affect the strength of conclusions, as smaller samples are more vulnerable to random fluctuations and may fail to reflect the broader heterogeneity of immune responses across populations. Second, antibody binding evaluations were restricted to anti-WT S protein; comprehensive multiplex assays targeting various spike subdomains and multiple variants are warranted to better compare responses between the A-A and I-I-I groups. Addressing these shortcomings will require future multicenter studies incorporating larger participant numbers and rigorous, parallel evaluations of different vaccine platforms in authentic epidemiological settings to strengthen reliability and broader applicability.

Conclusion

The present retrospective cohort analysis reveals that an Ad5-boosted SARS-CoV-2 vaccine offers superior safeguarding against symptomatic BA.5 breakthrough infection, achieved through integrated adaptive and innate immune mechanisms. Expression of native S protein by this platform is linked to heightened production of cross-reactive neutralizing antibodies effective against both WT and BA.5 lineages, concurrently with the induction of NK cells exhibiting trained immunity characteristics. These results demonstrate the advantages of the Ad5 vector platform over inactivated vaccines in orchestrating layered, multifaceted immune defenses against BA.5. Going forward, vaccine design efforts should favor strategies that successfully merge extensive humoral coverage with innate immune training, thereby better preparing for the emergence of novel variants and potential Disease X pathogens.

Acknowledgments: None

Conflict of Interest: None

Financial Support: None

Ethics Statement: None

References

1. Fu D, He G, Li H, Tan H, Ji X, Lin Z, et al. Effectiveness of COVID-19 vaccination against SARS-CoV-2 Omicron variant infection and symptoms—China, December 2022–February 2023. China CDC Wkly. 2023;5(17):369.
2. Farina SF, Gao GP, Xiang ZQ, Rux JJ, Burnett RM, Alvira MR, et al. Replication-defective vector based on a chimpanzee adenovirus. J Virol. 2001;75(23):11603-13.
3. Löser P, Hofmann C, Both GW, Uckert W, Hillgenberg M. Construction, rescue, and characterization of vectors derived from ovine atadenovirus. J Virol. 2003;77(22):11941-51.

4. Lioznov D, Amosova I, Sheetikov SA, Zornikova KV, Serdyuk Y, Efimov GA, et al. Immunogenicity and safety of a recombinant adenovirus type-5 COVID-19 vaccine in adults: data from a randomised, double-blind, placebo-controlled, single-dose, phase 3 trial in Russia. PLoS ONE. 2023;18(3):e0278878.
5. Zhu FC, Guan XH, Li YH, Huang JY, Jiang T, Hou LH, et al. Immunogenicity and safety of a recombinant adenovirus type-5-vectored COVID-19 vaccine in healthy adults aged 18 years or older: a randomised, double-blind, placebo-controlled, phase 2 trial. Lancet. 2020;396(10249):479-88.
6. Halperin SA, Ye L, MacKinnon-Cameron D, Smith B, Cahn PE, Ruiz-Palacios GM, et al. Final efficacy analysis, interim safety analysis, and immunogenicity of a single dose of recombinant novel coronavirus vaccine (adenovirus type 5 vector) in adults 18 years and older: an international, multicentre, randomised, double-blinded, placebo-controlled phase 3 trial. Lancet. 2022;399(10321):237-48.
7. Sadoff J, Gray G, Vandebosch A, Cárdenas V, Shukarev G, Grinsztejn B, et al. Safety and efficacy of single-dose Ad26.COV2.S vaccine against Covid-19. N Engl J Med. 2021;384(23):2187-201.
8. Logunov DY, Dolzhikova IV, Shcheblyakov DV, Tukhvatulin AI, Zubkova OV, Dzharullaeva AS, et al. Safety and efficacy of an rAd26 and rAd5 vector-based heterologous prime-boost COVID-19 vaccine: an interim analysis of a randomised controlled phase 3 trial in Russia. Lancet. 2021;397(10275):671-81.
9. Li JX, Wu SP, Guo XL, Tang R, Huang BY, Chen XQ, et al. Safety and immunogenicity of heterologous boost immunisation with an orally administered aerosolised Ad5-nCoV after two-dose priming with an inactivated SARS-CoV-2 vaccine in Chinese adults: a randomised, open-label, single-centre trial. Lancet Respir Med. 2022;10(8):739-48.
10. Li JX, Hou LH, Gou JB, Yin ZD, Wu SP, Wang FZ, et al. Safety, immunogenicity and protection of heterologous boost with an aerosolised Ad5-nCoV after two-dose inactivated COVID-19 vaccines in adults: a multicentre, open-label phase 3 trial. Lancet Infect Dis. 2023;23(10):1143-52.
11. Huang T, Zhang S, Dai DF, Wang BS, Zhuang L, Huang HT, et al. Safety and immunogenicity of heterologous boosting with orally aerosolised or intramuscular Ad5-nCoV vaccine and homologous boosting with inactivated vaccines (BBIBP-CorV or CoronaVac) in children and adolescents: a randomised, open-label, parallel-controlled, non-inferiority, single-centre study. Lancet Respir Med. 2023;11(8):698-708.
12. Zhao X, Qiu T, Huang X, Mao Q, Wang Y, Qiao R, et al. Potent and broadly neutralizing antibodies against sarbecoviruses induced by sequential COVID-19 vaccination. Cell Discov. 2024;10(1):14.
13. Cromer D, Steain M, Reynaldi A, Schlub TE, Wheatley AK, Juno JA, et al. Neutralising antibody titres as predictors of protection against SARS-CoV-2 variants and the impact of boosting: a meta-analysis. Lancet Microbe. 2022;3(1):e52-61.
14. Goga A, Bekker LG, Garrett N, Reddy T, Yende-Zuma N, Fairall L, et al. Breakthrough SARS-CoV-2 infections during periods of delta and omicron predominance, South Africa. Lancet. 2022;400(10348):269-71.
15. Malato J, Ribeiro RM, Leite PP, Casaca P, Fernandes E, Antunes C, et al. Risk of BA.5 infection among persons exposed to previous SARS-CoV-2 variants. N Engl J Med. 2022;387(10):953-4.
16. Barnes E, Folgori A, Capone S, Swadling L, Aston S, Kurioka A, et al. Novel adenovirus-based vaccines induce broad and sustained T cell responses to HCV in man. Sci Transl Med. 2012;4(115):115ra1.
17. Marquez-Martinez S, Vijayan A, Khan S, Zahn R. Cell entry and innate sensing shape adaptive immune responses to adenovirus-based vaccines. Curr Opin Immunol. 2023;80:102282.
18. Grinshtein N, Yang TC, Parsons R, Millar J, Denisova G, Dissanayake D, et al. Recombinant adenovirus vaccines can successfully elicit CD8+ T cell immunity under conditions of extreme leukopenia. Mol Ther. 2006;13(2):270-9.
19. Netea MG, Joosten LA. Beyond adaptive immunity: induction of trained immunity by COVID-19 adenoviral vaccines. J Clin Invest. 2023;133(2):e166467.
20. Murphy DM, Cox DJ, Connolly SA, Breen EP, Brugman AAI, Phelan JJ, et al. Trained immunity is induced in humans after immunization with an adenoviral vector COVID-19 vaccine. J Clin Invest. 2023;133(2):e162581.
21. Ge MQ, Ho AW, Tang Y, Wong KH, Chua BY, Gasser S, et al. NK cells regulate CD8+ T cell priming and dendritic cell migration during influenza A infection by IFN-γ and perforin-dependent mechanisms. J Immunol. 2012;189(5):2099-109.
22. Gao N, Jennings P, Yuan D. Requirements for the natural killer cell-mediated induction of IgG1 and IgG2a expression in B lymphocytes. Int Immunol. 2008;20(5):645-57.

23. Rahman MA, de Silva Castro I, Schifanella L, Bissa M, Franchini G. Vaccine induced mucosal and systemic memory NK/ILCs elicit decreased risk of SIV/SHIV acquisition. Front Immunol. 2024;15:1441793.
24. Palgen JL, Tchitchek N, Huot N, Elhmouzi-Younes J, Lefebvre C, Rosenbaum P, et al. NK cell immune responses differ after prime and boost vaccination. J Leukoc Biol. 2019;105(5):1055-73.
25. Zhao Z, Tingting C, Mingzhu H, Shuo L, Xiaoling S, Guichang L, et al. Heterologous boosting with third dose of coronavirus disease recombinant subunit vaccine increases neutralizing antibodies and T cell immunity against different severe acute respiratory syndrome coronavirus 2 variants. Emerg Microbes Infect. 2022;11(1):829-40.
26. Andrews S. FastQC: a quality control tool for high throughput sequence data [Internet]. Babraham Bioinformatics; 2010. Available from: https://www.bioinformatics.babraham.ac.uk/projects/fastqc
27. Martin M. Cutadapt removes adapter sequences from high-throughput sequencing reads. EMBnet.journal. 2011;17(1):10.
28. Mudge JM, Carbonell-Sala S, Diekhans M, Martinez JG, Hunt T, Jungreis I, et al. GENCODE 2025: reference gene annotation for human and mouse. Nucleic Acids Res. 2024;53(D1):D966-75.
29. Kolberg L, Raudvere U, Kuzmin I, Adler P, Vilo J, Peterson H. g:Profiler—interoperable web service for functional enrichment analysis and gene identifier mapping (2023 update). Nucleic Acids Res. 2023;51(W1):W207-12.
30. Tang D, Chen M, Huang X, Zhang G, Zeng L, Zhang G, et al. SRplot: a free online platform for data visualization and graphing. PLoS One. 2023;18(11):e0294236.
31. Manso T, Folch G, Giudicelli V, Jabado-Michaloud J, Kushwaha A, Nguefack Ngoune V, et al. IMGT® databases, related tools and web resources through three main axes of research and development. Nucleic Acids Res. 2022;50(D1):D1262-72.
32. Gao B, He L, Bao Y, Chen Y, Lu G, Zhang Y, et al. Repeated vaccination of inactivated SARS-CoV-2 vaccine dampens neutralizing antibodies against Omicron variants in breakthrough infection. Cell Res. 2023;33(3):258-61.
33. Pal R, Ferrari MG, Honda-Okubo Y, Wattay L, Caple J, Navarrete J, et al. Study of immunogenicity and efficacy against Omicron BA.5 of recombinant protein-based COVID-19 vaccine delivered by intramuscular and mucosal routes in nonhuman primates. Vaccine. 2024;42(5):1122-35.
34. Garcia-Beltran WF, St. Denis KJ, Hoelzemer A, Lam EC, Nitido AD, Sheehan ML, et al. mRNA-based COVID-19 vaccine boosters induce neutralizing immunity against SARS-CoV-2 Omicron variant. Cell. 2022;185(3):457-66.e4.
35. Kawasuji H, Morinaga Y, Tani H, Saga Y, Yamada H, Yoshida Y, et al. Neutralizing antibody response of the wild-type/Omicron BA.1 bivalent vaccine as the second booster dose against Omicron BA.2 and BA.5. Microbiol Spectr. 2023;11(2):e05131-22.
36. Pan Y, Jia Z, Yu X, Lv H, Zhang Y, Wu Y, et al. Study on SARS-CoV-2 infection in middle-aged and elderly population infected with hepatitis virus: a cohort study in a rural area of northeast China. PeerJ. 2025;13:e19021.
37. Mendonça SA, Lorincz R, Boucher P, Curiel DT. Adenoviral vector vaccine platforms in the SARS-CoV-2 pandemic. NPJ Vaccines. 2021;6(1):97.
38. Logunov DY, Dolzhikova IV, Zubkova OV, Tukhvatulin AI, Shcheblyakov DV, Dzharullaeva AS, et al. Safety and immunogenicity of an rAd26 and rAd5 vector-based heterologous prime-boost COVID-19 vaccine in two formulations: two open, non-randomised phase 1/2 studies from Russia. Lancet. 2020;396(10255):887-97.
39. Dong D, Song Y, Wu S, Wang B, Peng C, Kong W, et al. Molecular basis of Ad5-nCoV Vaccine-Induced Immunogenicity. bioRxiv [Preprint]. 2024 [cited 2026 Aug 1]; 2024.06.21.600005. doi:10.1101/2024.06.21.600005
40. Travieso T, Li J, Mahesh S, Mello JDFRE, Blasi M. The use of viral vectors in vaccine development. NPJ Vaccines. 2022;7(1):75.
41. Bruhn M, Obara M, Chiyyeadu A, Costa B, Salam A, Ziegler A, et al. Memory B cells anticipate SARS-CoV-2 variants through somatic hypermutation. J Infect. 2024;88(1):57-60.
42. Doria-Rose NA, Joyce MG. Strategies to guide the antibody affinity maturation process. Curr Opin Virol. 2015;11:137-47.

43. Xiang H, Zhao Y, Li X, Liu P, Wang L, Wang M, et al. Landscapes and dynamic diversifications of B-cell receptor repertoires in COVID-19 patients. Hum Immunol. 2022;83(2):119-29.
44. Yan Q, Hou R, Huang X, Zhang Y, He P, Zhang Y, et al. Shared IGHV1-69-encoded neutralizing antibodies contribute to the emergence of L452R substitution in SARS-CoV-2 variants. Emerg Microbes Infect. 2022;11(1):2749-61.
45. Xiao S, Yu L, Lei Y, Guang Y, Min Q. Neutralizing antibodies targeting SARS-CoV-2 spike protein. Stem Cell Res. 2020;50:102125.
46. Yuan M, Liu H, Wu NC, Lee CC, Zhu X, Zhao F, et al. Structural basis of a shared antibody response to SARS-CoV-2. Science. 2020;369(6507):1119-23.
47. Wang Y, Yuan M, Lv H, Peng J, Wilson IA, Wu NC. A large-scale systematic survey reveals recurring molecular features of public antibody responses to SARS-CoV-2. Immunity. 2022;55(6):1105-17.
48. Yuan M, Wilson IA. Major classes of neutralizing antibodies evaded by the SARS-CoV-2 Omicron variant. Structure. 2023;31(7):755-7.
49. Björkström NK, Lindgren T, Stoltz M, Fauriat C, Braun M, Evander M, et al. Rapid expansion and long-term persistence of elevated NK cell numbers in humans infected with hantavirus. J Exp Med. 2010;208(1):13-21.
50. Biron CA, Byron KS, Sullivan JL. Severe herpesvirus infections in an adolescent without natural killer cells. N Engl J Med. 1989;320(26):1731-5.
51. Wagstaffe HR, Mooney JP, Riley EM, Goodier MR. Vaccinating for natural killer cell effector functions. Clin Transl Immunol. 2018;7(1):e1010.
52. Kar UK, Joosten LAB. Training the trainable cells of the immune system and beyond. Nat Immunol. 2020;21(2):115-9.
53. Lam E, Falck-Pedersen E. Unabated adenovirus replication following activation of the cGAS/STING-dependent antiviral response in human cells. J Virol. 2014;88(24):14426-39.
54. Cox A, Cevik H, Feldman HA, Canaday LM, Lakes N, Waggoner SN. Targeting natural killer cells to enhance vaccine responses. Trends Pharmacol Sci. 2021;42(9):789-801.